Localization, Physiology, and Modulation of a Molluskan Dopaminergic Synapse

Neil S. Magoski,* Andrew G. M. Bulloch

Department of Physiology and Biophysics and Neuroscience Research Group, Faculty of Medicine, University of Calgary, 3330 Hospital Drive NW, Calgary, Alberta T2N 4N1, Canada

Received 12 October 1996; accepted 24 April 1997

ABSTRACT: **We investigated the location, physiology, and modulation of an identified synapse from the central nervous system (CNS) of the mollusk *Lymnaea stagnalis*. Specifically, the excitatory synapse from interneuron right pedal dorsal one (RPeD1) to neurons visceral dorsal two and three (VD2/3) was examined. The gross and fine morphology of these neurons was determined by staining with Lucifer yellow or sulforhodamine. In preparations where RPeD1 was stained with Lucifer yellow and VD2/3 with sulforhodamine, the axon collaterals occupied similar regions, suggesting that these neurons make physical contact in the CNS. Digital confocal microscopy of these preparations revealed that presynaptic varicosities made apparent contact (synapses) with smooth postsynaptic axon collaterals. The number of putative synapses per preparation was about five to 10. Regarding physiology, the synaptic latency was moderately rapid at 24.1 ± 5.2 ms. Previous work indicated that RPeD1 uses dopamine as a neurotransmitter. The RPeD1 → VD2/3 excitatory postsynaptic potential (EPSP) and the VD2/3 bath-applied dopamine (100-μM) response displayed a similar decrease in input resistance and a similar predicted reversal potential (−31 vs. −26 mV), indicating that the synapse and exogenous dopamine activate the same conductance. Finally, bath-applied serotonin (10 μM) rapidly and reversibly depressed the RPeD1 → VD2/3 synapse but did not affect the VD2/3 bath-applied dopamine (100-μM) response, suggesting a presynaptic locus of action for serotonin. The effect of serotonin was not associated with any changes to the pre- or postsynaptic membrane potential and input resistance, or the presynaptic action potential half-width. The RPeD1 → VD2/3 synapse provides an opportunity to examine the anatomy and physiology of transmission, and is amenable to the study of neuromodulation.** *J Neurobiol* 33: 247–264, 1997

Keywords: **invertebrate; mollusk; *Lymnaea stagnalis*; identified neurons; chemical synapse; double label; contact; serotonin; modulation**

INTRODUCTION

The molluskan central nervous system (CNS) has been used extensively to investigate chemical synaptic transmission and plasticity (Kandel, 1979; Bulloch, 1989; Bulloch and Ridgway, 1989). This includes studies on the CNS from the freshwater snail *Lymnaea stagnalis* (Boer et al., 1987; Kits et al., 1991). Identified *Lymnaea* neurons have proved useful in determining the synaptic relationships between specific neurons (McCrohan and Benjamin, 1980; Benjamin and Winlow, 1981; Benjamin, 1984; Skingsley et al., 1993), as well as elucidating their behavioral roles (Janse et al., 1985; Buckett et al., 1990; Syed and Winlow, 1991; Yeoman et al., 1993; Kemenes and Elliott, 1994). However, in this system there remains a lack of both fundamental anatomical and physiological information regarding specific chemical connections. For example, despite the identification of many connections in *Lymnaea*, the actual location and site(s) of transmission in the CNS for any *identified* synapse is unknown. With respect to physiology, for the majority of synapses the effect of pre- and postsynaptic membrane

* Present address: Department of Pharmacology, School of Medicine, Yale University, New Haven, CT 06520

Correspondence to: A. G. M. Bulloch

Contract grant sponsor: Medical Research Council of Canada

 CCC 0022-3034/97/030247-18

potential on transmission have not been fully examined. Also, when the transmitter at a synapse is known, a systematic comparison of the transmitter-evoked response to that of the synaptic response is often lacking. Finally, with the exception of the feeding network, relatively little work has been performed regarding potential neuromodulators such as serotonin (Kandel and Schwartz, 1982) in *Lymnaea*.

In the present study, the morphology, physiology, and modulation of an identified chemical synapse in the CNS of *L. stagnalis* were investigated. The aim was to provide a thorough documentation of the properties of an identified synapse that can be used for subsequent investigations. The presynaptic neuron was a dopaminergic, respiratory interneuron known as right pedal dorsal one (RPeD1), and the postsynaptic cells were giant neurons, visceral dorsal two and three (VD2/3). This synapse was previously documented by Benjamin and Winlow (1981) and has been used to study aspects of dopaminergic transmission (Magoski et al., 1995) and synapse formation (Magoski et al., 1993). Furthermore, these neurons are tractable and readily identifiable, and the presence of their connection is relatively reliable. Thus, additional information on these neurons will prove valuable in exploiting them for future work on transmission and plasticity. Regarding morphology, in an attempt to locate synapses, neurons RPeD1 and VD2/3 were stained with the contrasting intracellular dyes Lucifer yellow and sulforhodamine, and examined with digital confocal microscopy. To better understand synaptic transmission in *Lymnaea*, several parameters of transmission were investigated. These included synaptic latency, an examination of the influence of pre- and postsynaptic voltage, and a comparison between the synaptic and dopamine-evoked responses in VD2/3. Finally, serotonin, a well-known neuromodulator with a long history of study in molluskan neurobiology (Kandel and Schwartz, 1982; Mackey et al., 1989; Katz and Frost, 1995; Byrne and Kandel, 1996), was examined for its ability to acutely modulate the RPeD1 → VD2/3 synapse.

MATERIALS AND METHODS

Animals

The experiments employed a stock of the mollusk, *L. stagnalis* (Gastropoda, Pulmonata, Basommatophora, Lymnaeidae), raised and maintained at the University of Calgary. Animals had shell lengths of 15–25 mm (age ~ 1–4 months).

Dissection and Saline

Prior to dissection, the shell was removed with scissors; the animal was then pinned to the silicone rubber base (General Electric RTV 616) of a dissecting tray. A superficial midsagittal incision was made along the dorsal surface, exposing the CNS for subsequent removal. For electrophysiology, the CNS was pinned to the rubber base of a small-volume (~500-μL) recording chamber. For intracellular dye staining, the CNS was pinned to a small rubber pad. The CNS was pinned out dorsal surface up, with the cerebral commissure cut so that the CNS lay flat. Animal dissection and pinning out of the CNS was performed in normal *Lymnaea* saline (composition in m*M*: NaCl 51.3, KCl 1.7, $CaCl_2$ 4.1, $MgCl_2$ 1.5, and Hepes 5.0; adjusted to pH 7.9 with 1 *N* NaOH). Electrophysiology was performed in high-Ca^{2+}/high-Mg^{2+} saline (composition in m*M:* NaCl 51.3, KCl 1.7, $CaCl_2$ 24.6, $MgCl_2$ 1.5, $MgSO_4$ 7.5, and Hepes 5.0; pH 7.9). This saline reduces the probability of polysynaptic effects by raising the threshold for action potentials in putative interneurons (Austin et al., 1967; Berry and Pentreath, 1976; Elliott and Benjamin, 1989). Salts were obtained from Sigma or BDH (Canada). Experiments were performed at room temperature (18–20°C).

Electrophysiology

Single-barrel borosilicate micropipettes (World Precision Instruments; TW 150F-6) were used. When filled with 2

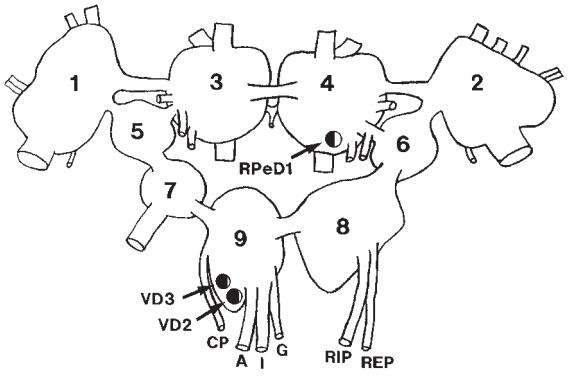

Figure 1 Schematic neuronal map of *Lymnaea*'s central ring ganglia. The ganglia are numbered according to Syed and Winlow (1991): left and right cerebral (1,2); left and right pedal (3,4); left and right pleural (5,6); left and right parietal (7,8); and visceral (9); the buccal ganglia are not shown. The cerebral commissure has been cut and the cerebral ganglia placed to the side, ventral surface up, so the CNS is essentially flat, with the rest of the ganglia being dorsal surface up. Black shading denotes white coloration in the cells; no shading indicates orange coloration. Cutaneous pallial = CP; anal = A; intestinal = I; genital = G; right internal parietal = RIP; right external parietal = REP. Identified neurons: right pedal dorsal one (RPeD1); visceral dorsal two (VD2); visceral dorsal three (VD3).

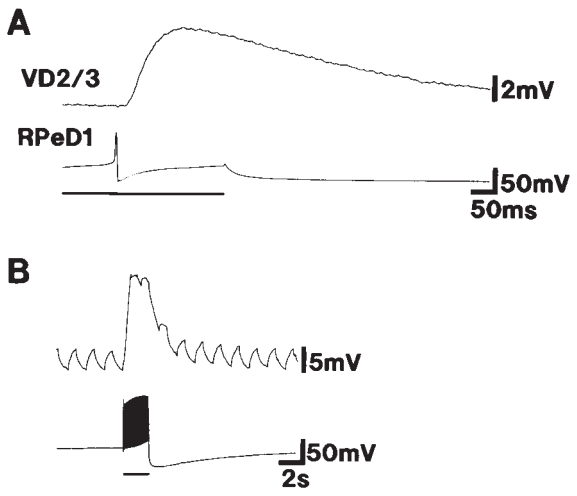

Figure 2 Latency and changes to postsynaptic input resistance of the RPeD1 → VD2/3 synapse. (A) When recorded at high speed, a 20-ms action-potential-to-EPSP inflection latency was observed. Membrane potentials: RPeD1 = −50 mV; VD2/3 = −70 mV. (B) Neuron VD2/3 showed a decrease in membrane resistance during a compound EPSP. This can been seen as a reduction in the voltage deflections produced by the injection of hyperpolarizing current pulses during the EPSP. In experiments not shown, transient depolarization (2–3 s and magnitudes similar to the EPSP) of VD2/3 produced only a minor (10–20%) reduction in membrane resistance. Membrane potentials: RPeD1 = −55 mV; VD2/3 = −70 mV. Bars indicate the duration of depolarizing current injection into RPeD1.

M potassium acetate, the electrodes had final resistances of 20–30 MΩ. The back end of the electrodes was filled with a small amount of mineral oil (Sigma; M5904) to reduce both noise and evaporative loss of electrolyte. Data were collected with a Neurodata 8100 dual-channel intracellular amplifier equipped with a bridge balance. Microelectrodes were connected to the amplifier headstages via silver wires coated with chloride. Another silver wire coated with chloride served as ground. The voltage was displayed on a Tektronix 5113 dual-beam storage oscilloscope and recorded on a Gould 2200S 2 channel chart recorder. In some cases, the voltage was also recorded on a Nicolet 201 digital storage oscilloscope. Electrodes were balanced, prior to and following impalement, with 20-ms, 1-nA-square, hyperpolarizing current pulses delivered by a Grass S88 stimulator and isolation unit. To manipulate the membrane potential, current was injected into a neuron via the direct current injection function on the amplifier. On some occasions, it was necessary to facilitate microelectrode penetration of neurons in the CNS by exposing the surrounding sheath to a small pronase crystal (Sigma type XIV), held by forceps, for 1–3 s. If this was performed, the CNS was then rinsed five times in cold (~4°C) normal saline to remove excess enzyme. The chamber was perfused with high-Ca^{2+}/high-Mg^{2+} saline at a rate of ~3 mL/min using a Fisher 3132 Microperpex peristaltic pump.

Drugs were delivered to neurons by bath application. Either dopamine (6-hydroxydopamine, H6507; Sigma) or serotonin (5-hydroxytryptamine, H7752; Sigma) was dissolved in high-Ca^{2+}/high-Mg^{2+} saline containing 0.01% (w/v) Fast green (Sigma F7258), and the solution was introduced into the bath via a three-way valve system. The solution also contained 0.1% (w/v) sodium metabisulfite (Sigma S1516) to prevent oxidation. When Fast green and sodium metabisulfite were applied alone, no discernable effect on membrane potential, action potential wave form, firing pattern, or synaptic transmission was observed.

Intracellular Dye Staining

The morphology of single and synaptically paired neurons in the CNS was examined using Lucifer yellow and

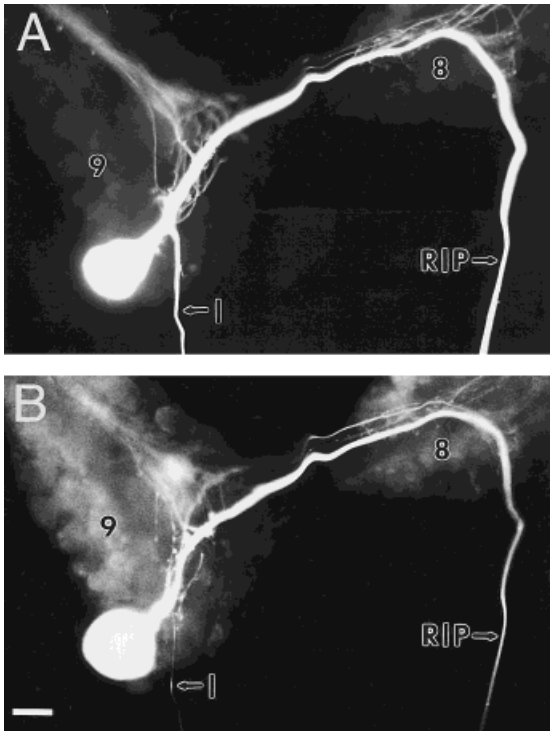

Figure 3 A dual label of the two neurons that constitute VD2/3. (A) A Lucifer yellow–stained VD2/3 had a main axon which projected from the visceral ganglion to the right parietal ganglion, with secondary axons projecting through the intestinal and right internal parietal nerves. Axon collaterals extended from the main axon in the right parietal and visceral ganglia. (B) In the same preparation, the other cell of the VD2/3 pair was stained with sulforhodamine and had an identical morphology. The axon collaterals were less obvious with the rhodamine stain; this is likely a function of the dye. The field of view is the same for (A) and (B), with the calibration bar being equivalent to 75 μm. Pertinent ganglia are numbered as follows: right parietal (8); visceral (9). Intestinal = I; right internal parietal = RIP.

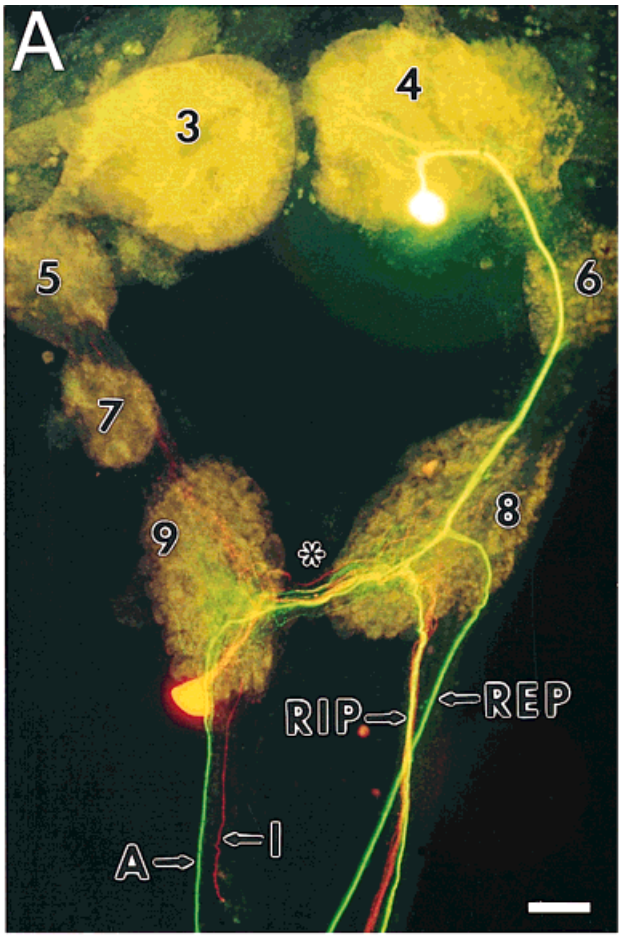

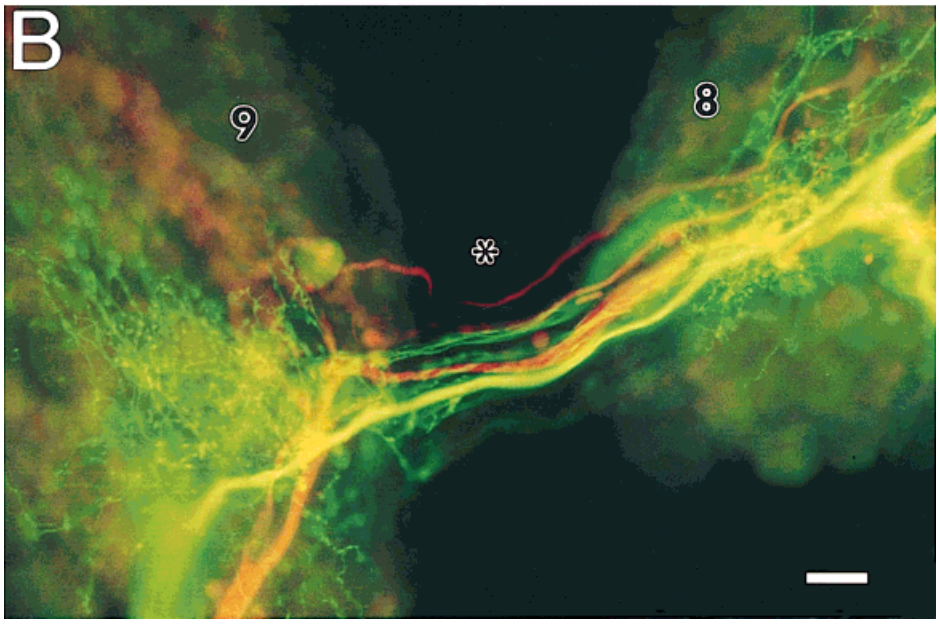

Figure 4 Dual-labeled RPeD1 and VD2/3. (A) A Lucifer yellow–stained RPeD1 (yellow neuron) had a main axon projecting from the right pedal ganglion to the right parietal and visceral ganglia. This axon diverged into three secondary axons projecting through the anal, right internal parietal, and right external parietal nerves. Axon collaterals extended from the main axon in the right pedal, right parietal, and visceral ganglia. A sulforhodamine-stained

sulforhodamine staining. For Lucifer yellow staining, microelectrode tips were filled with a 4% (w/v) solution of Lucifer yellow CH, lithium salt (Molecular Probes; L453) dissolved in 0.1% (w/v) LiCl, and the microelectrode was then backfilled with 0.1% LiCl. Lucifer yellow was injected with constant 0.5–1.0-nA hyperpolarizing current for 5–30 min. A neuron was considered stained with Lucifer yellow when the soma fluoresced brightly under a blue filter (Schott; BG12) mounted on the dissection microscope. For sulforhodamine staining, microelectrode tips were filled with a 3% (w/v) solution of sulforhodamine 101 (Molecular Probes; S359) dissolved in distilled water, and the microelectrode shaft was then backfilled with 0.5 *M* KCl. Sulforhodamine was injected with one to 10 pressure pulses (2 s on at 3.5 kg/cm^2 and 3 s off) applied via a Medical Systems PPS2 pneumatic pressure unit. A neuron was considered stained with sulforhodamine when it appeared dark purple under normal illumination. Once stained, the preparations were left overnight at 4°C in normal saline, and then fixed for 3 h in 3.7% (v/v) formaldehyde (BDH; B28421) in phosphate buffer (132.3 m*M* Na_2HPO_4 and 25.2 m*M* $NaH_2PO_4 \times H_20$; pH 7.3). The CNS were then dehydrated in a series of ethanol washes: 50%, 70%, 90%, and 100% ethanol (2 × 30 min). The CNS was defatted for 10 min in dimethyl sulfoxide (Sigma D5879), then cleared and mounted in methyl salicylate (Sigma; M6752). Stained neurons were viewed on a Zeiss Universal microscope using epifluorescence, with Neofluar (×6.3 and ×10) and Plan-Neofluar objectives (×16 and ×25). For Lucifer yellow, a 436/8-nm bandpass excitation filter, both 500-nm-long pass and 600-nm-short pass barrier filters, and a 510-nm dichroic mirror were used. For sulforhodamine, a 546/12-nm band pass excitation filter, a 590-nm-long pass barrier filter, and a 580-nm dichroic mirror were used. Photomicrographs were taken with 400 ASA slide and 50 ASA negative film.

Digital Confocal Microscopy

To examine neuronal morphology in greater detail, and to locate regions of putative synaptic contact between pre- and postsynaptic neurons, digital confocal microscopy was performed on dye-stained neurons. A Universal microscope was fitted with a motorized, computer-controlled stage (Ludl Electronic Products) and a Kodak Megaplus 1.6 computer-controlled, charged-coupled device camera. The filter sets and mirrors used were the same as for conventional microscopy. The program Slices (written by Dr. Michael Schoel, University of Calgary) controlled the stage and camera to acquire digitized confocal images (optical slices). Throughout the acquisition, the camera remained stationary while the stage (and preparation) was moved in 1-μm steps away (into focus) from the objective (Plan Neofluar, ×25, water immersion, 0.8 numeric aperture). A series of optical slices was gathered for an area of the preparation using one of the filter sets, and if necessary, the same series was collected again using the second filter set. Thus, a single region that was identical in *X*, *Y*, and *Z* coordinates could be imaged using both the Lucifer yellow and rhodamine filter sets. For a series of multiple images, the only variable during the acquisition was the *Z* coordinate. Following aquisition, each image was processed by the program Clrdpxls (written by Dr. Schoel) to remove aberrant pixels. During the acquisition the camera failed to digitize a small number of pixels (<1%); these appeared either as pure white or pure black in the image. The Clrdpxls program removed the aberrant pixels by taking the average intensity of the surrounding nine pixels and assigning the aberrant pixel that intensity. The out-of-focus haze was then removed from the images using the program Micro-Tome 3.0 (Vaytek). Finally, using Adobe Photoshop 2.5 (Adobe Systems), the images were adjusted for brightness and contrast, psuedocolored, and, if necessary, overlapped (red onto green).

Statistical Analysis

The program Instat 2.01 (GraphPad Software) was used to calculate the mean and standard error of the mean of each data point and to run the following statistical tests: paired Student *t* test and repeated-measures analysis of variance (ANOVA) with Bonferroni's multiple comparisons post hoc test. Data were considered significantly different when $p < 0.05$; the *p* value was two-tailed. Inplot 4.03 was used to plot line and bar graphs, and to fit linear regression lines.

RESULTS

The RPeD1 → VD2/3 Synapse

The present study examined the excitatory monosynaptic connection from interneuron RPeD1 to

VD2/3 (red neuron) had a main axon which projected from the visceral ganglion to the right parietal ganglion, with secondary axons projecting through the intestinal and right internal parietal nerves. Axon collaterals extended from the main axon in the right parietal and visceral ganglia. Calibration bar = 150 μm. (B) The same preparation at higher magnification, with a view of the visceral and right parietal ganglia and their adjoining connective (asterisk). The axons and axon collaterals of both pre- and postsynaptic neurons occupy similar regions in both the neuropile and within the connective. Calibration bar = 40 μm. In this and all subsequent dual-labeled preparations, RPeD1 made an excitatory synapse onto VD2/3. Ganglia are numbered as follows: left pedal (3); right pedal (4); left pleural (5); right pleural (6); left parietal (7); right parietal (8); visceral (9). Anal = A; intestinal = I; right internal parietal = RIP; right external parietal = REP.

Table 1 Axonal Projections of RPeD1 and VD2/3

Neuron	Presence of Axon in Nerve (%)[1]					
	CP	A	I	G	RIP	REP
RPeD1 (*n*/*N*)[2]	4% (2/48)	100% (48/48)	17% (8/48)	21% (10/48)	100% (48/48)	100% (48/48)
VD2/3 (*n*/*N*)	1% (1/93)	8% (7/93)	100% (93/93)	0% (0/93)	100% (93/93)	3% (3/93)

[1] Nerves originating from the visceral and right parietal ganglia are abbreviated as follows: cutaneous pallial = CP; anal = A; intestinal = I; genital = G; right internal parietal = RIP; right external parietal = REP. See Figure 1 for the location of these nerves. A 100% value indicates that an axon was always found in the nerve; a 0% value indicates that an axon was never found in the nerve; and a value between 0 and 100% indicates that a variable number of preparations had axons in the nerve.

[2] The number of particular observations (*n*) out of the total number of preparations (*N*) is given in brackets below the percentage. The data represent neurons stained with either Lucifer yellow or sulforhodamine.

neurons VD2/3 (Fig. 1). Although VD2/3 are two separate neurons, they are indistinguishable on the basis of position, size, color, or electrophysiology; consequently, as suggested by Benjamin and Winlow (1981), they are referred to as VD2/3. The presence of this synapse has been previously documented (Winlow and Benjamin, 1977, 1981) and determined to be monosynaptic (Winlow et al., 1981), but a detailed analysis of its morphology, physiology, or modulation has not been performed. Previous work using immunohistochemical (Elekes et al., 1991; Werkman et al., 1991), chromatographic, and pharmacologic criteria (Magoski et al., 1995) demonstrated that the RPeD1 → VD2/3 synapse is dopaminergic. In the present study, the synapse was moderately fast, with an action potential-to-excitatory postsynaptic potential (EPSP) inflection latency of 24.1 ± 5.2 ms ($n = 27$) (Fig. 2). When two EPSPs were elicited consecutively, the latency of the first EPSP was not significantly different from that of the second (25.4 ± 6.1 ms vs. 25.6 ± 7.2 ms, respectively; $n = 7$; $p > 0.05$, paired Student *t* test; latency was measured using a triggered response on a digital oscilloscope and defined as the time from the peak of the action potential to the estimated inflection point of the initial phase of the PSP). In addition, the EPSP was associated with a decreased membrane resistance in VD2/3 ($n = 5$) (Fig. 2).

Morphology of RPeD1 and VD2/3

The axonal projections and axon collaterals of RPeD1 and VD2/3 were characterized using intracellular staining of either single neurons with Lucifer yellow, or two neurons with a combination of Lucifer yellow and sulforhodamine. The basic morphology of RPeD1 was examined previously by Haydon and Winlow (1981), but is described in greater detail here. On the other hand, the morphology of VD2/3 has not been previously described. When both of the neurons that constitute VD2/3 were dual-labeled, the neurons typically had the same morphology with respect to axon projections and axon collaterals (Fig. 3). A dual label of RPeD1 and VD2/3 is shown in Figure 4. The two dyes revealed that the axons and axon collaterals of the pre- and postsynaptic neurons occupied, in part, the same regions of the visceral and right parietal ganglia–potential regions for contact.

Regarding axonal projections, the neurons exhibited both invariable and variable axonal projections through various visceral and right parietal nerves (Table 1). For VD2/3, axons were always observed in the intestinal and right internal parietal nerves; sometimes in the cutaneous pallial, anal, and right external parietal nerves; and never in the genital nerve. Neuron VD2/3 had arbors of axon collaterals in the visceral and right parietal ganglia, which sometimes extended as far as the right and left pleural ganglia. Neuron RPeD1 always had an axon in the anal, right internal parietal, and right external parietal nerves. On a few occasions, RPeD1 also projected axons through the cutaneous pallial, intestinal, and genital nerves. Neuron RPeD1 displayed arbors of axon collaterals, extending from the main axon, in the visceral, right parietal, and right pedal ganglia. Axonal variability could be an artifact of staining, although it seems unlikely, because the percentages of variant axons are low over many preparations.

To examine the structure of the axon collaterals, digital confocal microscopy was applied to either single Lucifer yellow–stained RPeD1 ($n = 4$) or VD2/3 ($n = 4$). The optical sections in these cases were taken mainly from within the neuropile, and two types of collaterals were always observed. For both RPeD1 and VD2/3, some of these collaterals displayed varicosities running along their length; other collaterals were smooth and did not possess varicosities (Fig. 5). Both types of collaterals occurred in the same preparation, often in close prox-

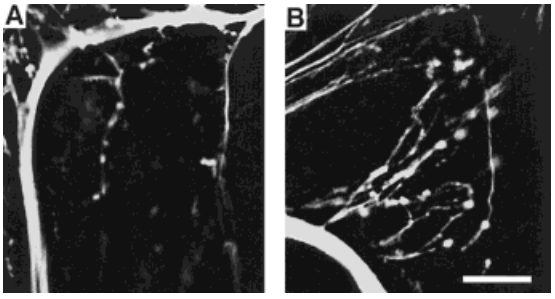

Figure 5 Digital confocal images of a region from a single Lucifer yellow–stained neuron. (A) An image of RPeD1 in the posterior lateral portion of the visceral ganglion. The main axon was evident as a large, bright process projecting across and down the field of view. The collateral on the left possessed obvious varicosities running along its length. The collateral on the right was relatively smooth. (B) An image of VD2/3 in the middle of the right parietal ganglion. The main axon can be seen as a large, bright process projecting across the bottom left-hand corner of the field of view. Several of the axon collaterals extended from the main axon toward the center of the field of view and possessed obvious varicosities running along their length. There were also a number of smooth collaterals that can be seen in the upper left-hand corner of the field of view. The calibration bar applies to both (A) and (B), and is equivalent to 20 μm.

imity, and in all ganglia where a particular neuron displayed collaterals. Collaterals were typically not observed in the same optical sections as the somata, i.e., in regions dorsal to the neuropile.

Putative Synapses between RPeD1 and VD2/3

In an attempt to localize and quantify synapses, digital confocal microscopy was applied to the dual-labeled preparations. In five separate preparations, all of which showed a physiologic excitatory synapse from RPeD1 to VD2/3, four or more potential contact sites were observed between the axon collaterals of a Lucifer yellow–stained RPeD1 and a sulforhodamine-stained VD2/3. In these cases, a single Lucifer yellow–labeled structure, quite possibly a presynaptic terminal, appeared to be just adjacent to, above, or below a sulforhodamine-labeled structure. In some examples, it was clear that the varicosities of RPeD1 were in juxtaposition with a smooth collateral of VD2/3 [Fig. 6(A)]. In other instances, the nature of the presynaptic element was less obvious, and may or may not have been varicose; however, the postsynaptic structure again appeared to be a smooth collateral [Fig. 6(B)]. The putative contact sites were observed in optical sections from within the neuropile in regions from either the right parietal ($n = 2$) or the visceral ($n = 3$) ganglia. The number of putative contacts for the five preparations were four, six, six, eight, and 10.

Physiology of the RPeD1 → VD2/3 Synapse and the VD2/3 Dopamine Response

The RPeD1 → VD2/3 synapse displayed paired-pulse facilitation. The facilitation was unusual in that the initial EPSP of a pair (elicited by two successive action potentials) often varied in magnitude with respect to the initial EPSP of other pairs; however, the overall magnitude of the faciliated EPSP did not vary within a preparation (Fig. 7). Given this, the majority of quantitative analyses on the synapse were carried out on the second of two EPSPs (as measured from baseline) evoked by paired-pulse stimulation.

The dependence of the amplitude of the VD2/3 EPSP on the membrane potential of RPeD1 was examined. As RPeD1 was hyperpolarized in 10-mV steps, from −50 to −90 mV, with the membrane potential of VD2/3 being maintained at a constant value, the EPSP magnitude did not change appreciably [Fig. 8(A)]. In a plot of EPSP magnitude versus presynaptic voltage, the linear regression gave a statistically straight line that was not significantly different from a slope of zero ($p > 0.05$; $n = 7$) [Fig. 8(B)]. Next, the dependence of the EPSP on the membrane potential of VD2/3 was tested. As VD2/3 was hyperpolarized in 10-mV steps from −40 to −90 mV, the EPSP increased in a linear fashion [Fig. 9(A)]. In a plot of EPSP magnitude versus postsynaptic voltage, the linear regression gave a predicted reversal potential of −26 mV ($n = 6$) [Fig. 9(B)]. Note that for the range of voltages tested on both RPeD1 and VD2/3, significant changes in membrane resistance were not observed while holding either of the cells for long periods of time (>1 min) at the various potentials.

If RPeD1 uses dopamine at this synapse, then the EPSP and the VD2/3 response to applied dopamine should share similar physiological properties. Like the EPSP, the VD2/3 bath-applied dopamine (100-μM) response exhibited a decrease in input resistance ($n = 7$) (Fig. 10). When VD2/3 was held at −40 mV, bath-applied dopamine (100 μM) produced spiking; holding the cell at more negative membrane potentials resulted in a steadily increased depolarization to bath-applied dopamine ($n = 7$)

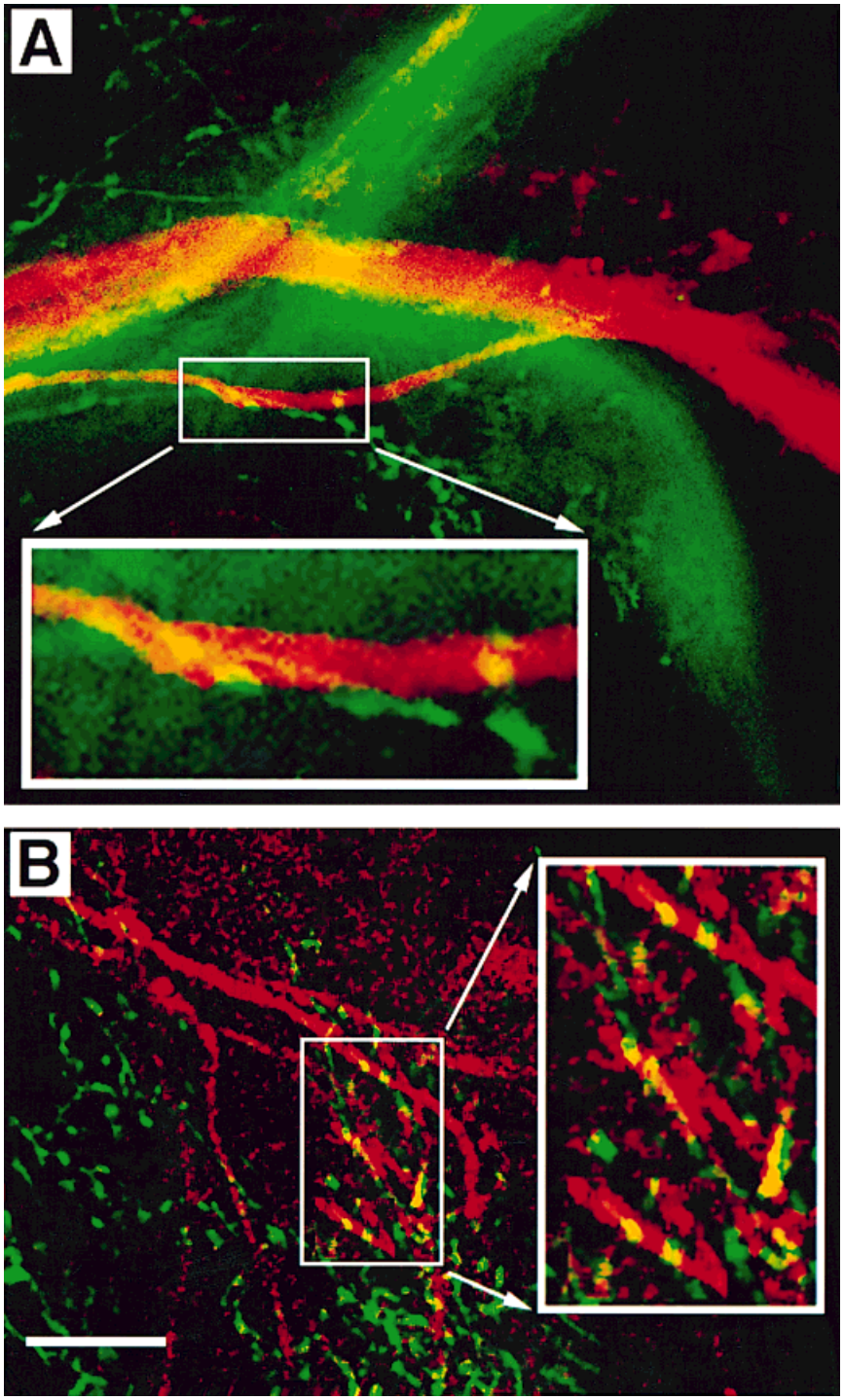

Figure 6 Putative synaptic contact sites between RPeD1 and VD2/3. (A) Digital confocal images of a Lucifer yellow–stained RPeD1 and a sulforhodamine-stained VD2/3 that have been pseudocolored and superimposed. The field of view is in the middle of the right parietal ganglion. The main and secondary axons of RPeD1 are the large green bands of out-of-focus haze, and the main axon of VD2/3 is the large, bright red process that projects across the middle of the field of view. A region displaying putative contact sites is enclosed in the small box. This region was magnified and is displayed in the enlarged box. At least four green-labeled varicosities of RPeD1 appeared to make contact with the smooth red-labeled axon collateral of VD2/3. Note that the main axons of both RPeD1 and VD2/3 were particularly

(Fig. 11). The linear regression of this relationship predicted a reversal potential of −31 mV (Fig. 12). When the relationship between the membrane potential of VD2/3 and both the RPeD1 → VD2/3 EPSP (from Fig. 9) and the VD2/3 dopamine response were plotted together, the predicted reversal potentials were similar (Fig. 12).

Serotonin Depresses the RPeD1 → VD2/3 Synapse

The final aspect of the study investigated the serotonergic modulation of this connection. To test if serotonin modulates the RPeD1 → VD2/3 synapse, the VD2/3 EPSP was measured before, during, and after exposure to serotonin. During a brief (3–5-min) exposure to serotonin (10 μM), the RPeD1 → VD2/3 EPSP was significantly depressed by an average of 71% ($n = 22$; $p < 0.001$, repeated-measures ANOVA; $p < 0.001$, Bonferroni's multiple comparisons test) [Figs. 13(A) and 14(A)]. The serotonin-induced synaptic depression was rapidly and fully reversible. The time course for the actions of serotonin was relatively rapid, with an onset time of 1.6 ± 0.2 min, a time to maximal effect of 2.8 ± 0.5 min, and a time to full recovery of 4.6 ± 0.8 min. Furthermore, the modulatory effect of serotonin was also dose dependent. At 100 μM ($n = 10$), serotonin depressed the synapse completely, while at 1 μM ($n = 4$), serotonin had no effect on the EPSP.

To test if serotonin was acting postsynaptically, the response of VD2/3 to bath-applied dopamine was measured before, during, and after exposure to serotonin. Serotonin did not effect the response of VD2/3 to bath-applied dopamine (100 μM; $n = 13$; $p > 0.05$, repeated-measures ANOVA) [Figs. 13(B) and 14(B)], suggesting a presynaptic locus of action.

As shown above, synaptic transmission at the RPeD1 → VD2/3 synapse can be affected by the physiological properties of the postsynaptic neuron. The effect of serotonin (10 μM) on the membrane potential, input resistance, and action potential half-width (often a determinant of transmitter release) was examined (Fig. 15). Serotonin did not significantly alter the membrane potential of either RPeD1 or VD2/3 ($n = 22$; $p > 0.05$, repeated-measures ANOVA). Furthermore, the input resistance of RPeD1 was unaffected by serotonin ($n = 7$; $p > 0.05$, repeated-measures ANOVA). However, although the input resistance of VD2/3 remained unchanged during the exposure to serotonin ($n = 14$; $p > 0.05$, repeated-measures ANOVA), following wash, the input resistance of VD2/3 showed a significant and inexplicable increase ($n = 14$; $p < 0.0001$, repeated-measures ANOVA; $p < 0.001$, Bonferroni's multiple comparisons test). Finally, serotonin did not affect the action potential half-width of RPeD1 ($n = 9$; $p > 0.05$, repeated-measures ANOVA). Taken together with the preceding data, these observations indicate a presynaptic site for serotonin's actions.

DISCUSSION

Neuronal Morphology

The gross and fine morphology of a neuron are important characteristics in establishing its identity and function. Intracellular dyes such as Lucifer yellow or sulforhodamine have proved useful in mapping axonal projections and examining presynaptic terminals (Stewart, 1981). Both RPeD1 and VD2/3 project their axons through the nerves of the visceral and right parietal ganglia (Figs. 3 and 4, and Table 1). These nerves innervate organs such as the heart, pneumostome (respiratory pore), and kidney (Buckett et al., 1990; Syed et al., 1991). In keeping with its axonal projections, RPeD1 is known to be part of the respiratory circuit in Lymnaea (Syed *et al.*, 1990; Syed and Winlow, 1991) and is capable of initiating pneumostome movements (Park and Winlow, 1994). The morphology of RPeD1 has been described previously (Haydon and Winlow,

well stained; this and their close proximity resulted in some additional out-of-focus haze that could not be removed by the Micro-Tome program. (B) In a different preparation, the field of view is in the middle of the visceral ganglion and no main axons are visible. A region displaying putative contact sites is enclosed in the small box. This region was magnified and is displayed in the enlarged box. At least eight green-labeled structures, possibly varicosities, of RPeD1 appeared to make contact with several red-labeled axon collaterals of VD2/3. In this case, a contact site was defined as an instancein which a green structure overlapped with a red one to make a yellow area of 0.5 μm^2 or larger. The calibration bar applies to both (A) and (B) and is equivalent to 20 μm for the entire field of view, 6 μm for the enlarged box in (A), and 10 μm for the enlarged box in (B).

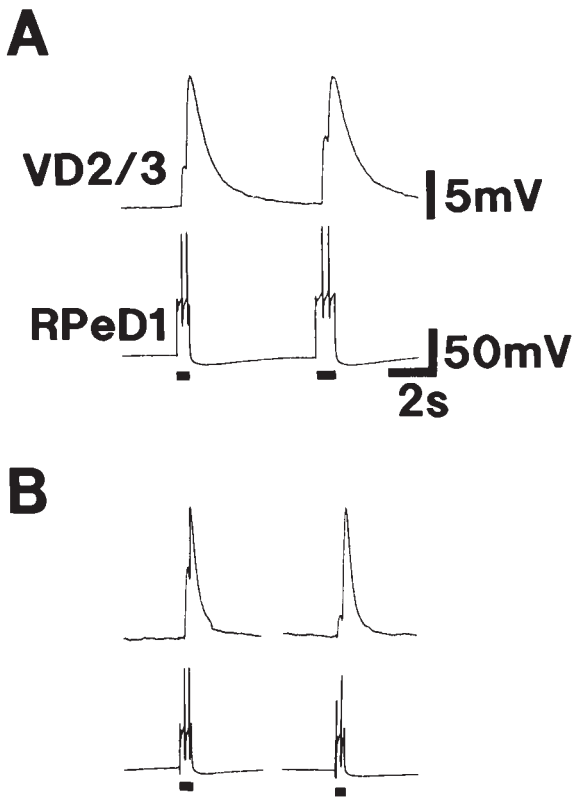

Figure 7 Paired-pulse facilitation in VD2/3. The paired-pulse facilitation varied with respect to the magnitude of the initial EPSP, but not with respect to the overall magnitude of the paired EPSP, i.e., the magnitude of the paired EPSP elicited by two successive action potentials was remarkably similar. (A) In this case, the initial EPSP of one paired EPSP was smaller than the initial EPSP of the subsequent paired EPSP, although the two dual EPSPs were equal. Membrane potentials: RPeD1 = −60 mV; VD2/3 = −90 mV. (B) In a different preparation (same calibration), the initial EPSP of one paired EPSP was larger than the initial EPSP of a subsequent paired EPSP, but again the two paired EPSPs were similar. The pairs of action potentials in RPeD1 were evoked by a single current pulse (at bar) rather than by two shorter pulses, because the latter method tended to fail in evoking a second action potential. Membrane potentials: RPeD1 = −65 mV; VD2/3 = −85 mV.

1981), and the results of the present work, including invariable and variable axons (see below), are consistent with that of the prior report. On the other hand, the morphology of VD2/3 has not been previously published, and the behavioral role of these neurons is unknown. However, VD2/3 consistently projects axons through the intestinal and right internal parietal nerves (Figs. 3 and 4), suggesting a visceral function.

The number and type of axonal projections of both RPeD1 and VD2/3 varied between preparations (Table 1). This is not surprising, for variations in the axonal projections of identified neurons have been previously reported for *Lymnaea* (Benjamin, 1976; Haydon and Winlow, 1981; Kyriakides et al., 1989; Magoski et al., 1994), *Helisoma* (Murphy and Kater, 1980), and *Aplysia* (Winlow and Kandel, 1976). Assuming these variant projections are established prior to adulthood, it is possible that they result from developmental plasticity (Winlow and Kandel, 1976). However, the functional consequence of such variable projections is unknown.

Digital confocal microscopy revealed that some of the axon collaterals from both RPeD1 and VD2/3 possessed varicosities, whereas others were smooth, presumably indicating pre- and postsynaptic sites (Fig. 7 and 8) (see below). Haydon and Winlow (1981) provided the first evidence of varicosities on single Lucifer yellow–labeled RPeD1 axon collaterals, but did not show varicosities from RPeD1

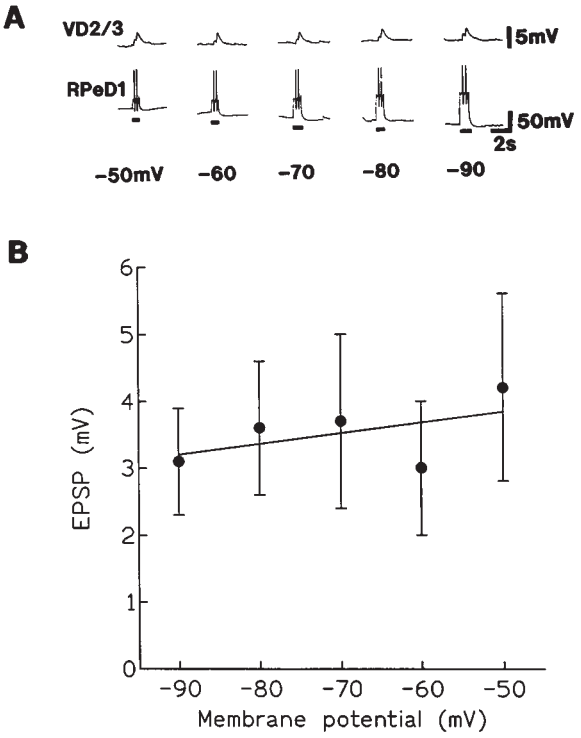

Figure 8 Effect of presynaptic membrane potential on the RPeD1 → VD2/3 EPSP. (A) Neuron RPeD1 was held at the designated membrane potentials, and an EPSP was elicited. As the presynaptic membrane potential was increased, the EPSP did not change. The membrane potential of VD2/3 was held at −80 mV. Bars indicate the duration of depolarizing current injection into RPeD1. (B) Relationship between RPeD1 membrane potential and the RPeD1 → VD2/3 EPSP. The average (n = 7) EPSP at presynaptic voltages from −40 to −90 mV was plotted. The linear regression of this plot gave a statistically straight line that was not significantly different from a slope of zero ($p > 0.05$).

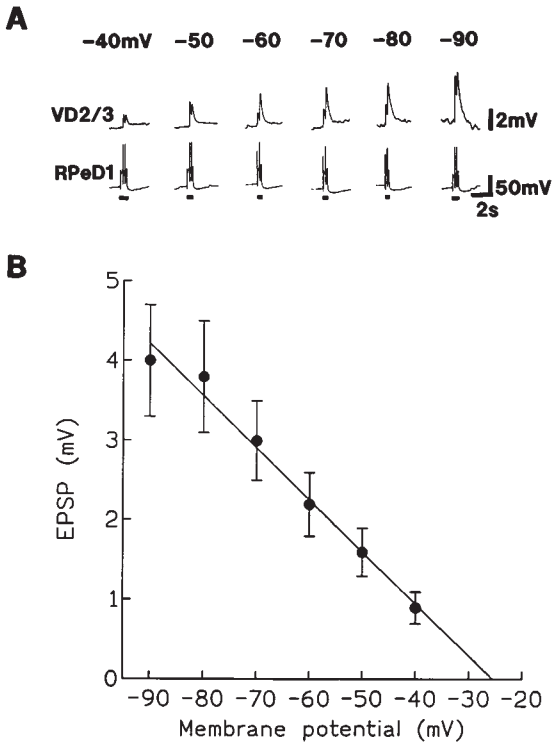

Figure 9 Effect of postsynaptic membrane potential on the RPeD1 → VD2/3 EPSP. (A) Neuron VD2/3 was held at the designated membrane potentials, and an EPSP was elicited. As the postsynaptic membrane potential was increased, the EPSP increased. The membrane potential of RPeD1 ranged from −50 to −55 mV. Bars indicate the duration of depolarizing current injection into RPeD1. (B) Relationship between VD2/3 membrane potential and the RPeD1 → VD2/3 EPSP. The average (n = 6) EPSP at postsynaptic voltages from −40 to −90 mV was plotted. The linear regression of this plot gave an estimated reversal potential of −26 mV.

in those ganglia where it has postsynaptic cells (i.e., the right parietal and visceral ganglia) and did not describe smooth versus varicose collaterals. Thus, it seemed worthwhile to further examine the issue of the morphology of axon collaterals. Notably, ultrastructural examination of the terminals in a homologous dopamine neuron in *Planorbis* showed them to be presynaptic terminals (Pentreath et al., 1974; Pentreath and Berry, 1975). In addition, electron microscopy of varicosities in *Aplysia* (Bailey et al. 1979) and the leech (Muller and McMahan, 1976) shows that they are presynaptic terminals. Data from the crayfish neuromuscular junction (Jahromi and Atwood, 1974) and vertebrate preparations, including rodents and humans (Smiley et al., 1992; Edwards, 1995), also indicates that varicosities are presynaptic terminals. Therefore, it is reasonable to propose that the varicosities from both RPeD1 and VD2/3 are also presynaptic terminals. Conversely, the smooth axon collaterals (Fig. 5) are possibly where postsynaptic sites are located.

Sites of possible synaptic contact between RPeD1 and VD2/3 were observed when confocal microscopy was performed on dual-labeled preparations (Fig. 6). In some cases, it was clear that in either the right parietal or the visceral ganglion, the varicosities of RPeD1 came into close apposition at discrete points with a smooth process of VD2/3 [Fig. 6(A)]. The contact sites are considered putative because the labeled structures are at the very least in the same optical section provided by the confocal system. Consequently, the collaterals are either very close or in physical contact with one another. This is consistent with the concept that the varicosities are presynaptic terminals which synapse onto nonvaricose collaterals. All contact sites were in the neuropile, where synaptic transmission is believed to occur (Bullock and Horridge, 1965). Appropriately, electron microscopy of the CNS of *Lymnaea* (Roubos and Moorer-van Delft, 1979) and its close relative, *Helisoma* (Berdan et al., 1987), found true morphologic synapses only in the neuropile and not onto somata.

There are relatively few published data regarding contact between neurons presumed to be monosynaptically connected *in situ*. A light microscopy study in the leech indicated that the number of contacts between pre- and postsynaptic neurons can be as high as ∼100 (DeRiemer and Macagno, 1981); however, other studies suggest that contact sites can be fewer in number, such as the 30 to 40 contacts estimated between *Aplysia* sensory and motor neurons (Bailey et al., 1979), or the even smaller range of 1 to ∼10 in the hippocampus (Sorra and Harris, 1993; Gulyas et al. 1993; Buhl et al., 1994). The RPeD1 → VD2/3 synapse appears to be in the lower

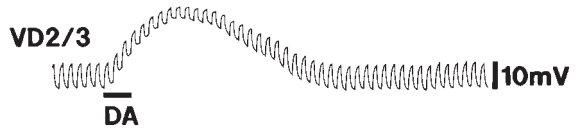

Figure 10 Changes in VD2/3 membrane resistance during a bath-applied dopamine response. Neuron VD2/3 showed a 50% decrease in membrane resistance during dopamine application (100 μM, at the bar, for 10 s). This can been seen as a reduction in the voltage deflections, produced by the injection of hyperpolarizing current pulses, during the dopamine response. In experiments not shown, sustained depolarization (30–60 s and magnitudes similar to the dopamine response) of VD2/3 produced no obvious reduction in membrane resistance. VD2/3 membrane potential = −90 mV. DA = dopamine.

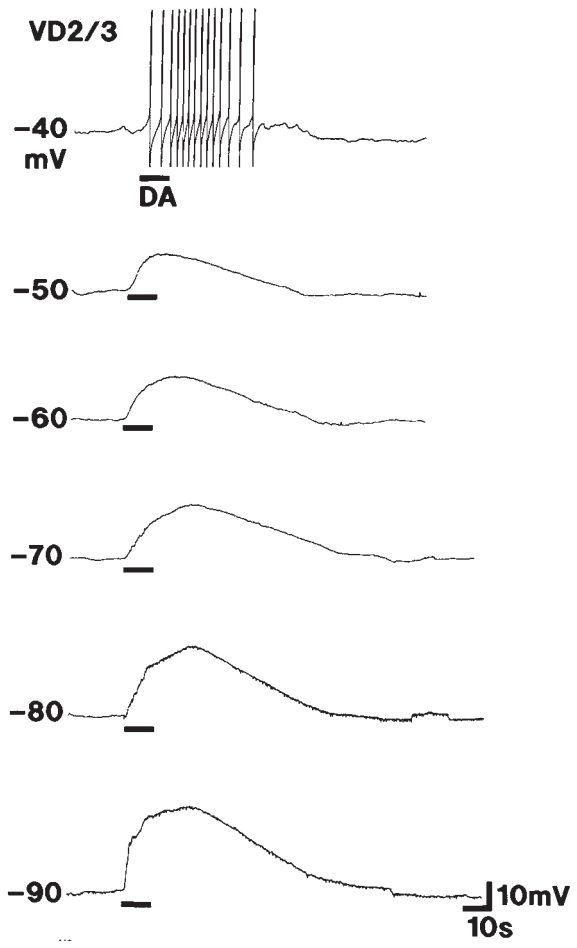

Figure 11 Effect of membrane potential on the VD2/3 bath-applied dopamine response. Neuron VD2/3 was held at different membrane potentials (given at the left-hand side) and dopamine (100 μM) was bath-applied (at the bar). As the membrane potential was increased, the dopamine response increased. The concentration of 100 μM dopamine is slightly above the ED_{50} of the dose–response curve (Magoski et al., 1995) and was chosen because it produced a reliable and readily quantitated response. DA = dopamine.

end of the range, with ~5–10 contacts/preparation. There could have been more contact sites which were not observed or were not detectable because of incomplete dye staining. The fact that RPeD1 and VD2/3 were synaptically and likely physically connected supports previous indications that these neurons are monosynaptically connected (Winlow et al., 1981).

Physiology of Synaptic Transmission

Previous investigators have established that the RPeD1 → VD2/3 synapse is chemical and monosynaptic (Winlow et al., 1981). A constant and rapid latency is often considered a characteristic of a chemical synapse (Berry and Pentreath, 1975). Appropriately, the RPeD1 → VD2/3 synapse had a latency of ~25 ms (Fig. 2). The latency of VD2/3 EPSP was examined previously by Winlow et al. (1981); however, those investigators found a latency of ~40 ms, possibly because very large animals (up to 10 g) were used in that study. In such animals, RPeD1's axon would be much longer, possibly resulting in an increased soma-to-synapse action potential conduction time.

The RPeD1 → VD2/3 synapse displayed paired-pulse facilitation, a phenomenon not previously documented or described at this synapse. The faciliation was unusual in that the size of the initial EPSP varied but the absolute magnitude of the summed EPSP was constant. This may be due to Ca^{2+} buffering in the terminal which sets a ceiling for the level of free Ca^{2+} and limits the amount of Ca^{2+} avaliable to the secretory apparatus. Thus, no matter how much Ca^{2+} enters during the first action poten-

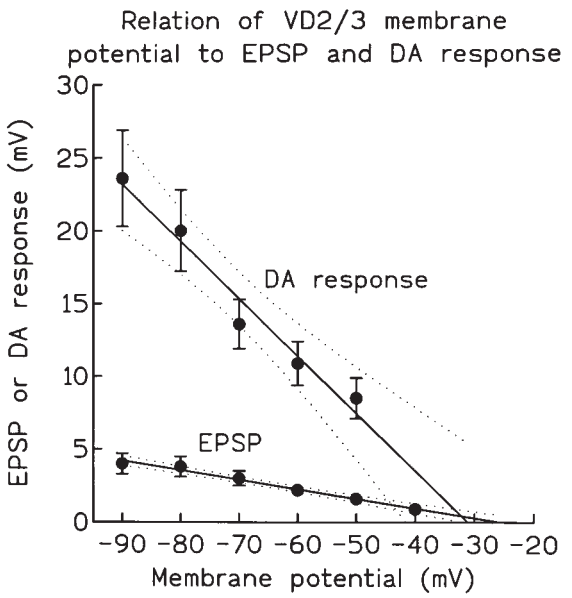

Figure 12 Relationship between VD2/3 membrane potential and both the RPeD1 → VD2/3 EPSP and VD2/3 bath-applied dopamine response. The data and linear regression of both the VD2/3 EPSP (from Fig. 9) and the dopamine response were plotted. The reversal potentials were −26 mV for the EPSP and −31 mV for the dopamine response. The 95% confidence intervals for the regression are given as dotted lines. These intervals overlap, suggesting that the reversal potentials are similar. The dramatic difference in slope of the two lines can be explained by the fact that the synapse presumably activates a relatively small number of dopamine receptors, while bath-applied dopamine activates a much larger number, including synaptic and extrasynaptic receptors.

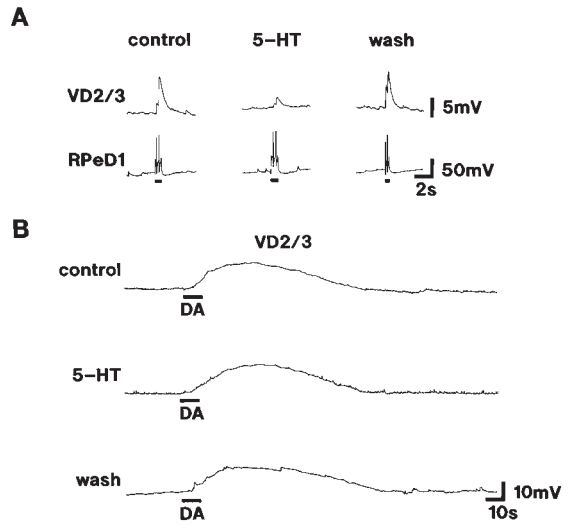

Figure 13 Serotonin depressed the RPeD1 → VD2/3 synapse but had no effect on the VD2/3 dopamine response. (A) Following a 3-min exposure to 10 μM serotonin, the RPeD1 → VD2/3 EPSP was depressed by ~75%. The effect of serotonin was fully reversible. Membrane potentials: RPeD1 = −54 mV; VD2/3 = −78 mV. (B) In the same preparation, the bath-applied dopamine (100 μM, at the bar) response in VD2/3 was not affected by serotonin. DA = dopamine; 5-HT = serotonin.

tial; the amount supplied during the second spike cannot elevate Ca^{2+} levels above the set point. This would lead to a fixed amount of transmitter release for two action potentials and result in a consistently summed EPSP.

In many preparations, the membrane potential of the presynaptic and/or postsynaptic soma can influence synaptic transmission. The postsynaptic soma potential strongly affected the magnitude of the VD2/3 EPSP (Fig. 9), while the presynaptic soma potential had no effect on the VD2/3 EPSP (Fig. 8). This would suggest that the postsynaptic soma is electrotonically closer to the synapse than the presynaptic soma. This is supported by anatomical data in which putative synapses are far closer to the postsynaptic than to the presynaptic soma (Fig. 6). It is somewhat unusual that the membrane potential of the presynaptic soma had little influence on the synapse. At synapses in the mollusks *Aplysia* (Shimahara and Peretz, 1978; Shapiro, 1980; Connor et al., 1986) and *Helisoma* (Coates and Bulloch, 1985), as well as the leech (Nicholls and Wallace, 1978), depolarization of the presynaptic soma increased, while hyperpolarization decreased, the PSP amplitude.

Previous studies have provided chemical (McCaman et al., 1979; Magoski et al., 1995), histological, or immunocytochemical (Cottrell et al., 1979; Audesirk, 1985; Werkman et al., 1991; Elekes et al., 1991) data demonstrating the presence of dopamine in the soma of RPeD1. Furthermore, Magoski et al. (1995) provided extensive pharmacologic evidence indicating that RPeD1 uses dopamine as a neurotransmitter at several synapses, including its connection with VD2/3. In the

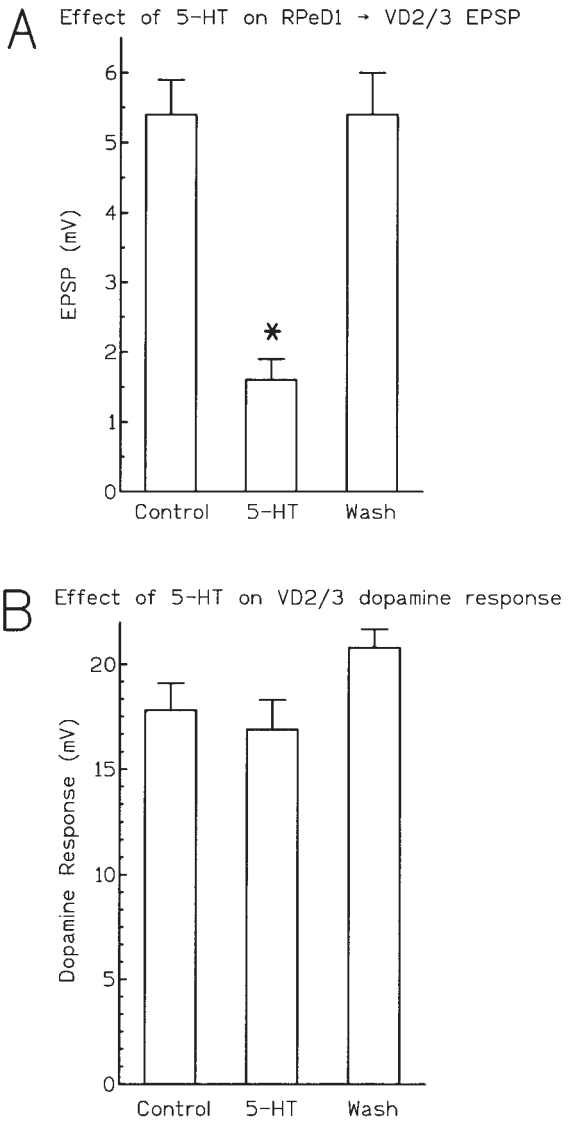

Figure 14 Effect of serotonin on the RPeD1 → VD2/3 EPSP and the VD2/3 bath-applied dopamine response. (A) Serotonin (10 μM) significantly and reversibly depressed the RPeD1 → VD2/3 EPSP. The asterisk indicates that the mean EPSP was significantly different from both the mean control and wash EPSP ($n = 22$; p 0.001, repeated-measures ANOVA; $p < 0.001$, Bonferroni's multiple comparisons test). (B) Serotonin (10 μM) did not have a significant effect on the VD2/3 bath-applied dopamine (100-μM) response ($n = 13$; $p > 0.05$, repeated-measures ANOVA). 5-HT = serotonin.

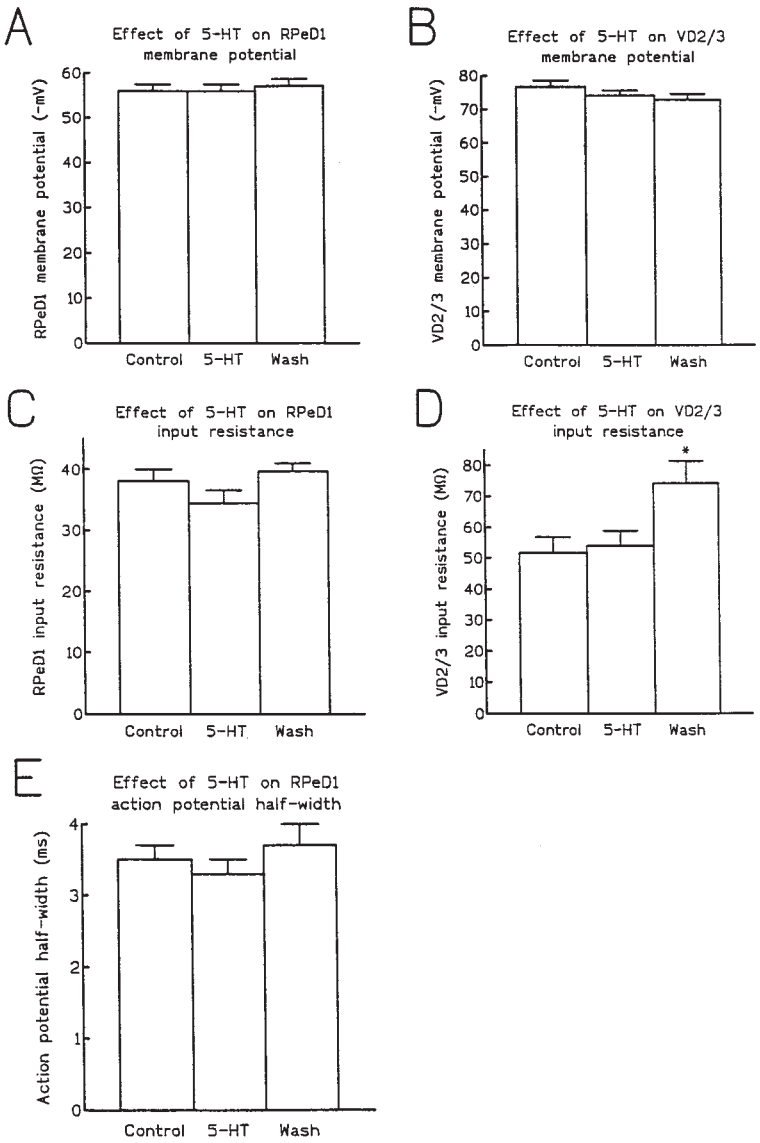

Figure 15 Tests for the effects of serotonin on the physiologic properties of the pre- and postsynaptic neurons. (A,B) Serotonin (10 μM) did not affect the membrane potential of either RPeD1 or VD2/3 ($n = 22$; $p > 0.05$, repeated-measures ANOVA). (C,D) Serotonin (10 μM) did not affect the input resistance of RPeD1 ($n = 7$; $p > 0.05$, repeated-measures ANOVA); however, following wash of serotonin, the input resistance of VD2/3 did show a significant increase, as indicated by the asterisk ($n = 14$; $p < 0.0001$, repeated-measures ANOVA; $p < 0.001$, Bonferroni's multiple comparisons test). (E) Serotonin (10 μM) did not affect the action potential half-width of RPeD1 ($n = 9$; $p > 0.05$, repeated-measures ANOVA). The action potential half-width was measured by first determining a point on the voltage sweep, 20 ms prior to the peak of the action potential. The voltage difference between this point and the peak of the action potential was halved and designated as the halfway point along the rising phase. The half-width was then determined by measuring the distance (time in ms) from the halfway point on the rising phase to a corresponding parallel point on the falling phase of the action potential. The 20-ms value used to determine the halfway point was chosen arbitrarily, in that it always resulted in the cursor being to the left of the inflection point of the rising phase.

present study, the RPeD1 → VD2/3 synapse was investigated further by examining the physiology of both the VD2/3 EPSP and dopamine response. The synaptic and dopamine response of VD2/3 both involved a decrease in input resistance [compare Figs. 2(A) and 10]. Furthermore, the reversal

potentials of the EPSP and the dopamine response in VD2/3 are similar (Fig. 12), suggesting that the synaptic input and dopamine activate the same conductance. Together with prior pharmacological data (Magoski et al., 1995), this supports the conclusion that dopamine is used as a neurotransmitter in RPeD1.

Serotonin-Induced Synaptic Depression

Serotonin is a transmitter and modulator in the molluskan nervous system (S.-Roza, 1984). It is abundant in the *Lymnaea* CNS (Cottrell et al., 1979; Audesirk, 1985; Croll and Chiasson, 1989) and is known to have a role in the control of feeding (McCrohan and Benjamin, 1980; Kyriakides and McCrohan, 1989). However, despite the long history of studying serotonergic modulation of synaptic transmission in mollusks (Kandel and Schwartz, 1982; Mackey et al., 1989; Katz and Frost, 1995), few experiments regarding serotonin as a modulator have been undertaken in *Lymnaea*. Given the role of RPeD1 in respiration (Syed and Winlow, 1991), knowledge regarding possible modulators of this neuron would prove useful in understanding how it is integrated into its circuit(s).

Serotonin had pronounced effects on transmission at the RPeD1 → VD2/3 synapse, rapidly depressing the EPSP [Figs. 13(A) and 14(A)]. The time course for the action of serotonin was in the range of a few minutes. In a previous study in *Lymnaea,* serotonin was found to depress the electrical synapse between two peptidergic neurons, with a very similar time course (Wildering and Janse, 1992). In other preparations, such as *Aplysia* abdomial ganglion (Pieroni and Byrne, 1992), crayfish neuromuscular junction (Dixon and Atwood, 1985), hamster superior colliculus (Mooney et al., 1994), or rat brain stem (Umemiya and Berger, 1995), serotonin also modulates transmission in a rapid manner. In most preparations, serotonin is thought to modulate transmission presynaptically. This was tested at the RPeD1 → VD2/3 synapse by examining the VD2/3 dopamine response before, during, and after serotonin exposure. While serotonin depressed the EPSP, it did not have a significant effect on the bath-applied dopamine response in VD2/3 [Figs. 13(B) and 14(B)], suggesting a presynaptic locus of action.

Serotonin modulates input resistance (excitability) and action potential shape in *Aplysia* neurons (Mercer et al., 1991; Byrne and Kandel, 1996) as well as input resistance in *Hermissenda* neurons (Schuman and Clark, 1994). However in *Lymnaea,* serotonin did not have a significant effect on the input resistance or membrane potential of either RPeD1 or VD2/3. Furthermore, the action potential half-width, a parameter that has been debated as a determinant of transmitter release in molluskan neurons (Klein, 1994), when measured in RPeD1 did not show a significant change during serotonin exposure (Fig. 15). When 5 m*M* tetraethylammonium chloride, a K^+ channel blocker that increases spike width and thereby makes the assay more sensitive, was added to the bath, serotonin again produced no change in half-width ($n = 4$; data not shown). However, there was a significant and inexplicable increase in VD2/3 input resistance during wash, following serotonin exposure. Collectively, the data suggest that serotonin depresses the synapse in a manner independent of basic electrophysiological properties. This is in contrast to a neuroglandular synapse in *Helisoma,* where FMRFamide depresses transmission by modulating both pre- and postsynaptic membrane potential and input resistance (Coates and Bulloch, 1985). Regarding the extensively studied serotonin-induced facilitation at the *Aplysia* sensory-to-motor neuron synapse, in that case, serotonin broadens the action potential, increases excitability, and alters the secretory machinery (Byrne and Kandel, 1996). While the depression seen at the *Lymnaea* synapse does not appear to involve changes to the spike or excitability, there is a possibility that serotonin decreases the sensitivity of the secretory apparatus to Ca^{2+} or decreases the mobilization of synaptic vesicles in the terminals of RPeD1.

There is a previous example of serotonin-induced synaptic depression in *Aplysia* (Rosen et al., 1989). In that case, serotonin depressed chemical transmission between a subclass of cerebral mechanoafferent neurons and their postsynaptic neurons, the cerebral B cells. Rosen et al. (1989) demonstrated that unlike the present case for *Lymnaea,* the depression was due to a narrowing of the presynaptic action potential duration. In other systems, serotonin has been shown to inhibit transmission at some lobster stomatogastric ganglion synapses (Johnson and Harris-Warrick, 1990; Johnson et al., 1995), sensory-to-motor neuron synapses in *Xenopus* (Sillar and Simmers, 1994), thalamosomatosensory synapses in rat (Rhoades et al., 1994), retinotectal synapses in hamster superior colliculus (Mooney et al., 1994), interneuronal-to-CA1 synapses in rat hippocampus (Schmitz et al., 1995), and interneuron-to-motor neuron synapses in rat hypoglossal nucleus (Umemiya and Berger, 1995). Thus, serotonin can be viewed as a neuromodulator within different neuronal systems and across different species.

CONCLUSIONS

A characterization of the location, physiology, and modulation of a synapse from neuron RPeD1 to neuron VD2/3 has been provided. Neuron RPeD1 makes an excitatory dopaminergic connection with VD2/3. This synapse appears to be localized to several discrete sites of contact between the axon collaterals of these neurons. The anatomical and physiological data strongly suggest that the RPeD1 → VD2/3 synapse is monosynaptic. Furthermore, the neuromodulator serotonin is capable of rapidly and reversibly depressing this connection. This information will prove useful in future investigations of synaptic transmission in the *Lymnaea* CNS.

The authors thank Garry Hauser for excellent technical assistance, and Nadine Ewadinger/Magoski for comments on earlier drafts of the manuscript. The authors also thank Dan-Bing Wang, Micheal Schoel, Micheal Hanzel, and David Basset-Jones for assistance with the confocal microscopy. This work was supported by grants from the Medical Research Council (MRC) of Canada (to AGMB). NSM was a recipient of MRC, Alberta Heritage Foundation for Medical Research (AHFMR), and NeuroScience Network of the Canadian Centres of Excellence Studentships. AGMB is an AHFMR Scientist.

REFERENCES

AUDESIRK, G. (1985). Amine-containing neurons in the brain of *Lymnaea stagnalis*: distribution and effects of precursors. *Comp. Biochem. Physiol.* **81A:**395–365.

AUSTIN, G., YAI, H. and SATO, M. (1967). Calcium ion effects on *Aplysia* membrane potentials. In: *Invertebrate Nervous Systems*, C. A. G. Wiersma, Ed. University of Chicago Press, Chicago, pp. 39–53.

BAILEY, C. H., THOMPSON, E. B., CASTELLUCCI, V. F., and KANDEL, E. R. (1979). Ultrastructure of the synapses of sensory neurons that mediate the gill-withdrawal reflex in *Aplysia. J. Neurocytol.* **8:**415–444.

BENJAMIN, P. R. (1976). Interganglionic variation in cell body location of snail neurones does not affect synaptic connections or central projections. *Nature* **260:**338–340.

BENJAMIN, P. R., and WINLOW, W. (1981). The distribution of three wide-acting synaptic inputs to identifed neurons in the isolated brain of *Lymnaea stagnalis* (L.). *Comp. Biochem. Physiol.* **70A:**293–307.

BENJAMIN, P. R. (1984). Interneronal network acting on snail neurosecretory neurones (yellow cells and yellow-green cells of *Lymnaea*). *J. Exp. Biol.* **113:**165–185.

BERDAN, R. C., SHIVERS, R. R., and BULLOCH, A. G. M. (1987). Chemical synapses, particle arrays, pseudogap junctions and gap junctions of neurons and glia in the buccal ganglion of *Helisoma. Synapse* **1:**304–323.

BERRY, M. S., and PENTREATH, V. W. (1976). Criteria for distinguishing between monosynapstic and polysynaptic transmission. *Brain Res.* **105:**1–20.

BOER, H. H., GERAERTS, W. P. M., and JOOSE, J. (1987). *Neurobiology Molluscan Models*, North Holland Press, Amsterdam.

BUCKETT, K. J., PETERS, M., and BENJAMIN, P. R. (1990). Excitation and inhibition of the heart of the snail, *Lymnaea*, by non-FMRFamidergic motoneurons. *J. Neurophysiol.* **63:**1436–1447.

BUHL, E. H., HALASY, K., and SOMOGYI, P. (1994). Diverse sources of hippocampal unitary inhibitory postsynaptic potentials and the number of synaptic release sites. *Nature* **368:**823–828.

BULLOCH, A. G. M. (1989). *The Cellular Basis of Neuronal Plasticity*, Manchester University Press, New York.

BULLOCH, A. G. M., and RIDGWAY, R. L. (1989). Neuronal plasticity in the adult invertebrate nervous system. *J. Neurobiol.* **20:**295–311.

BULLOCK, T. H., and HORRIDGE, G. A. (1965). *Structure and Function in the Nervous System of Invertebrates*, W. H. Freeman, San Francisco.

BYRNE, J. H., and KANDEL, E. R. (1996). Presynaptic facilitation revisited: state and time dependence. *J. Neurosci.* **16:**425–435.

COATES, C. J., and Bulloch, A. G. M. (1985). Synaptic plasticity in the molluscan peripheral nervous system: physiology and role for peptides. *J. Neurosci.* **5:**2677–2684.

CONNOR, J. A., KRETZ, R., and SHAPIRO, E. (1986). Calcium levels measured in a presynaptic neurone of *Aplysia* under conditions that modulate transmitter release. *J. Physiol.* **375:**625–642.

COTTRELL, G. A., ABERNETHY, B. K., and BARRAND, M. A. (1979). Large amine-containing neurones in the central ganglia of *Lymnaea stagnalis. Neuroscience* **4:**685–689.

CROLL, R. P., and CHIASSON, B. J. (1989). Postembryonic development of serotoninlike immunoreactivity in the central nervous system of the snail, *Lymnaea stagnalis*. *J. Comp. Neurol.* **280:**122–142.

DERIEMER, S. A., and MACAGNO, E. R. (1981). Light microscopic analysis of contacts between pairs of identified neurons with combined use of horseradish peroxidase and Lucifer yellow. *J. Neurosci.* **1:**650–657.

DIXON, D., and ATWOOD, H. L. (1985). Crayfish motor nerve terminal's response to serotonin examined by intracellular microelectrode. *J. Neurobiol.* **16:**409–424.

EDWARDS, F. A. (1995). Anatomy and electrophysiology of fast chemical synapses lead to a structural model for long-term potentiation. *Physiol. Rev.* **75:**759–787.

ELLIOTT, C. J. H., and BENJAMIN, P. R. (1989). Esophageal mechanoreceptors in the feeding system of the

pond snail *Lymnaea stagnalis*. *J. Neurophysiol.* **61:**727–736.

ELEKES, K., KEMENES, G., HIRIPI, L., GEFFARD, M., and BENJAMIN, P. R. (1991). Dopamine- immunoreactive neurones in the central nervous system of the pond snail *Lymnaea stagnalis. J. Comp. Neurol.* **307:**214–224.

GULYAS, A. I., MILES, R., SIK, A., TOTH, K., TAMAMAKI, N., and FREUND, T. F. (1993). Hippocampal pyramidal cells excite inhibitory neurons through a single release site. *Nature* **366:**683–687.

HAYDON, P. G., and WINLOW, W. (1981). Morphology of the giant dopamine-containing neuron, R.Pe.D.1, in *Lymnaea stagnalis* revealed by Lucifer yellow CH. *J. Exp. Biol.* **94:**149–157.

JAHROMI, S. S., and ATWOOD, H. L. (1974). Three-dimensional ultrastructure of the crayfish neuromuscular apparatus. *J. Cell Biol.* **63:**599–613.

JANSE, C., VAN DER WILT, G. J., VAN DER PLAS, J., and VAN DER ROEST, M. (1985). Central and peripheral neurones involved in oxygen perception in the pulmonate snail *Lymnaea stagnalis* (mollusca, gastropoda). *Comp. Biochem. Physiol.* **82A:**459–469.

JOHNSON, B. R., and HARRIS-WARRICK, R. M. (1990). Aminergic modulation of graded synaptic transmission in the lobster somatogastric ganglion. *J. Neurosci.* **10:**2066–2076.

JOHNSON, B. R., PECK, J. H., and HARRIS-WARRICK, R. M. (1995). Distributed amine modulation of graded chemical transmission in the pyloric network of the lobster somatogastric ganglion. *J. Neurophysiol.* **74:**437–452.

KANDEL, E. R. (1979). *Behavioral Biology of Aplysia.* Freeman, San Francisco.

KANDEL, E. R., and SCHWARTZ, J. H. (1982). Molecular biology of learning: modulation of transmitter release. *Science* **218:**433–443.

KATZ, P. S., and FROST, W. N. (1995). Intrinsic neuromodulation in the *Tritonia* swim CPG: the serotonergic dorsal swim interneurons act presynaptically to enhance transmitter release from interneuron C2. *J. Neurosci.* **15:**6035–6045.

KEMENES, G., and ELLIOTT, C. J. H. (1994). Analysis of the feeding motor pattern in the pond snail, *Lymnaea stagnalis*: photoinactivation of axonally stained pattern-generating interneurons. *J. Neurosci.* **14:**153–166.

KITS, K. S., BOER, H. H., and JOOSE, J. (1991). *Molluscan Neurobiology,* North Holland, Amsterdam.

KLEIN, M. (1994). Synaptic augmentation by 5-HT at rested *Aplysia* sensorimotor synapses: independence of action potential prolongation. *Neuron* **13:**159–166.

KYRIAKIDES, M., MCCROHAN, C. R., SLADE, C. T., SYED, N. I., and WINLOW, W. (1989). The morphology and electrophysiology of the paired pedal ganglia of *Lymnaea stagnalis* (L.). *Comp. Biochem. Physiol.* **93A**:861–876.

KYRIAKIDES, M. A., and MCCROHAN C. R. (1989). Effect of putatutive neuromodulators on rhythmic buccal motor output in *Lymnaea stagnalis. J. Neurobiol.* **20:**635–650.

MACKEY, S. L., KANDEL, E. R., and HAWKINS, R. D. (1989). Identified serotonergic neurons LCB1 and RCB1 in the cerebral ganglion of *Aplysia* produce presyaptic facilitation of siphon sensory neurons. *J. Neurosci.* **12:**4227–4235.

MAGOSKI, N. S., BAUCE, L. G., SYED, N. I., and BULLOCH, A. G. M. (1995). Dopaminergic transmission between identified neurons from the mollusc *Lymnaea stagnalis. J. Neurophysiol.* **74:**1287–1300.

MAGOSKI, N. S., SYED, N. I., and BULLOCH, A. G. M. (1993). Different conditions of *in vitro* synaptic contact produces different forms of synaptic transmission between identified neurons. *Soc. Neurosci. Abstr.* **19:**271.5.

MAGOSKI, N. S., SYED, N. I., and BULLOCH, A. G. M. (1994). A neuronal network from the mollusc *Lymnaea stagnalis*. *Brain Res.* **645:**201–214.

MCCAMAN, M. W., ONO, J. K., and MCCAMAN, R. E. (1979). Dopamine measurements in molluscan ganglia and neurons using a new, sensitive assay. *J. Neurochem.* **32:**1111–1113.

MCCROHAN C. R., and BENJAMIN, P. R. (1980). Synaptic relationships of the cerebral giant cells with motoneurones in the feeding system of *Lymnaea stagnalis. J. Exp. Biol.* **85:**169–186.

MERCER, A. R., EMPTAGE, N. J., and CAREW, T. J. (1991). Pharmacological dissociatin of modulatory effects of serotonin in *Aplysia* sensory neurons. *Science* **254**:1811–1813.

MOONEY, R. D., SHI, M. Y., and RHOADES, R. W. (1994). Modulation of retintectal transmission by presynaptic 5-HT_{1b} receptors in the superior colliculus of the adult hamster. *J. Neurophysiol.* **72:**3–13.

MULLER, K. J., and MCMAHAN, U. J. (1976). The shapes of sensory and motor neurones and the distribution of their synapses in ganglia of the leech: a study using intracellular injection of horse radish peroxidase. *Proc. R. Soc. Lond. B* **194**:481–499.

MURPHY, A. D., and KATER, S. B. (1980). Differential discrimination of appropriate pathways by regenerating identified neurons in *Helisoma*. *J. Comp. Neurol.* **190**:395–403.

NICHOLLS, J. G., and WALLACE, B. G. (1978). Modulation of transmission at an inhibitory synapse in the central nervous system of the leech. *J. Physiol.* **283:**357–369.

PARK, J.-H., and WINLOW, W. (1994). The neuronal basis of pneumostome movements in *Lymnaea. J. Physiol.* **476:**73P.

PENTREATH, V. W., and BERRY, M. S. (1975). Ultrastructure of the terminals of an identified dopamine-containing neurone marked by intracellular injection of radioactive dopamine. *J. Neurocytol.* **4:**249–260.

PENTREATH, V. W., BERRY, M. S., and COTTRELL, G. A. (1974). Anatomy of the giant dopamine-containing

neuron in the left pedal ganglion of *Planorbis corneus*. *Cell Tissue Res.* **151:**369–384.

PIERONI, J. P., and BYRNE, J. H. (1992). Differential effects of serotonin, FMRFamide, and small cardioactive peptide on multiple, distributed processes modulating sensorimotor synaptic transmission in *Aplysia*. *J. Neurosci.* **12:**2633–2647.

RHOADES, R. W., BENNETT-CLARKE, C. A., and SHI, M. Y. (1994). Effects of 5-HT on thalamocortical synaptic transmission in the developing rat. *J. Neurophysiol.* **72:**2438–2450.

ROUBOS, E. W., and MOORER-VAN DELFT, C. M. (1979). Synaptology of the central nervous system of the freshwater snail *Lymnaea stagnalis* (L.), with particular reference to neurosecretion. *Cell Tissue Res.* **198:**217–235.

S.-RÓZSA, K. (1984). The pharmacology of molluscan neurons. *Progr. Neurobiol.* **23:**79–150.

SCHMITZ, D., EMPSON, R. M., and HEINEMANN, U. (1995). Serotonin reduces inhibition via 5- HT_{1A} receptors in area CA1 of rat hippocampal slices *in vitro*. *J. Neurosci.* **15:**7217–7225.

SCHUMAN, E. M., and CLARK, G. A. (1994). Synaptic facilitation at connections of *Hermissenda* type B photoreceptors. *J. Neurosci.* **14:**1613–1622.

SHAPIRO, E., CASTELLUCCI, V. F., and KANDEL, E. R. (1980). Presynaptic membrane potential affects release in an identified neuron of *Aplysia* by modulating Ca^{2+} and K^+ currents. *Proc. Natl. Acad. Sci.* **77:**629–633.

SHIMAHARA, T., and PERETZ, B. (1978). Soma potential of an interneurone controls transmitter release in a monosynaptic pathway in *Aplysia*. *Nature* **273:**158–160.

SILLAR, K. T., and SIMMERS, A. J. (1994). Presynaptic inhibition of primary afferent transmitter release by 5-hydroxytryptamine at a mechanosensory synapse in the vertebrate spinal cord. *J. Neurosci.* **14:**2636–2647.

SKINGSLEY, D. R., BRIGHT, K., SANTAMA, N., VAN MINNEN, J., BRIERLEY, M. J., BURKE, J. F., and BENJAMIN, P. R. (1993). A molecularly defined cardiorespiratory interneuron expressing SDPFLRFamine/GDPFLRFamide in the snail *Lymnaea:* monosynaptic connections and pharmacology. *J. Neurophysiol.* **69:**915–927.

SMILEY, J. F., WILLIAMS, M., SZIGETI, K., GOLDMAN-RAKIC, P. S. (1992). Light and electron microscopic characterization of dopamine-immunoreactive axons in human cerebral cortex. *J. Comp. Neurol.* **321:**325–335.

SORRA, K. E., and HARRIS, K. M. (1993). Occurence and three-dimensional structure of multiple synapses between individual radiatum axons and their target pyramidal cells in hippocampal area CA1. *J. Neurosci.* **13:**3736–3748.

STEWART, W. W. (1981). Lucifer dyes—-highly fluorescent dyes for biological tracing. *Nature* **292:**17–21.

SYED, N. I., HARRISON, D., and WINLOW, W. (1991). Respiratory behavior in the pond snail *Lymnaea stagnalis* I. Behavioral analysis and the identification of motor neurons. *J. Comp. Physiol.* **169A:**541–555.

SYED, N. I., LUKOWIAK, K., and BULLOCH, A. G. M. (1990). In vitro reconstruction of the respiratory central pattern generator of the mollusk *Lymnaea*. *Science* **250:**282–285.

SYED, N. I., and WINLOW, W. (1991). Respiratory behavior in the pond snail *Lymnaea stagnalis* II. Neural elements of the central pattern generator (CPG). *J. Comp. Physiol.* **169A:**557–568.

UMEMIYA, M., and BERGER, A. J. (1995). Presynaptic inhibition by serotonin of glycinergic inhibitory synaptic currents in the rat brain stem. *J. Neurophysiol.* **73:**1192–1200.

WERKMAN, T. C., VAN MINNEN, J., VOORN P., STEINBUSCH, H. W. M., WESTERINK, B. H. C., DE VLIEGER, T. A., and STOOF, J. C. (1991). Localization of dopamine and its relation to the growth hormone producing cells in the central nervous system of the snail *Lymnaea stagnalis*. *Exp. Brain Res.* **85:**1–9.

WILDERING, W. C., and JANSE, C. (1992). Serotonergic modulation of junctional conductance in an identified pair of neurons in the mollusc *Lymnaea stagnalis*. *Brain Res.* **595:**343–352.

WINLOW, W., and BENJAMIN, P. R. (1977). Postsynaptic effects of a multiaction giant interneurone on identified snail neurones. *Nature* **268:**263–265.

WINLOW, W., HAYDON, P. G., and BENJAMIN, P. R. (1981). Multiple postsynaptic actions of the giant dopamine-containing neurone R.Pe.D.1 of *Lymnaea stagnalis*. *J. Exp. Biol.* **94:**137–148.

WINLOW, W., and KANDEL, E. R. (1976). The morphology of identified neurons in the abdominal ganglion of *Aplysia californica*. *Brain Res.* **112:**221–249.

YEOMAN, M. S., PARISH, D. C., and BENJAMIN, P. R. (1993). A cholinergic modulatory interneuron in the feeding system of the snail, *Lymnaea*. *J. Neurophysiol.* **70:**37–50.